WETTABILITY OF A SINGLE CARBON FIBER

Si Qiu[1,2], Carlos A. Fuentes[2], Dongxing Zhang[1,*], Aart Willem Van Vuure[2], David Seveno[2],

[1] School of Materials Science and Engineering, Harbin Institute of Technology, Harbin 150001, PR China
[2] Department of Materials Engineering, KU Leuven, Leuven 3001, Belgium

Keywords: Single carbon fiber, Wettability, Dynamic contact angles, Molecular-kinetic theory

ABSTRACT

Contact angle measurement, is a suitable method to characterize the wettability of a polymer matrix and reinforcing fibers, but it is highly challenging to measure the capillary force exerted by a probe liquid on a fiber accurately for very fine fibers like single carbon fibers. Therefore, we propose an innovative method for measuring dynamic contact angles with a tensiometer, considering both the intrinsic variability of the carbon fiber diameter and the extremely small amplitude of the capillary forces, allowing the measurement of reliable dynamic contact angles over a large range of contact line velocities. The analysis of the contact angle dynamics by the molecular-kinetic theory permits to check the relevancy of the measured contact angles and to obtain the static contact angle value, improving the prospect of employing tensiometry to better understand the wetting behavior of carbon fibers.

1 INTRODUCTION

The direct optical method and the Wilhelmy balance method are currently the two principal methods used to estimate the wettability of fibers. The latter one is a frequently used method which consists of measuring the capillary force exerted by a liquid on a solid substrate [1, 2]. However, testing the wettability of single carbon fibers with micron scale diameters is highly challenging as slight variations of the fiber diameter and the measured capillary forces can greatly influence the finally determined contact angles.

Moreover, the Wilhelmy method is a dynamic process with advancing (the fiber is dipped in the liquid) and receding (the fiber is withdrawn from the liquid) phases at a constant velocity. Meanwhile, the static advancing and receding contact angles are more relevant when calculating the components of the surface energy based on the Owens-Wendt [3] or Van Oss-Chaudhury methods [4]. Accordingly, much attention has been paid to the dynamic advancing contact angle at extremely low velocity whereas contact angle measurements at contact line velocities above 10mm/min have never been studied. From a theoretical point of view, dynamic contact angles can be analyzed using various approaches [5] even if it is widely accepted that the Molecular-kinetic theory (MKT) proposed by Blake [6] is able to describe eclectic liquid/solid systems. So far, studies dedicated to the dynamic wetting of carbon fibers are not available even if it is a key to the manufacturing of carbon fiber composites [7, 8].

In the present study, reliable and accurate water contact angles around single carbon fibers are reported. We propose a methodology which permits to measure dynamic contact angles taking into consideration both the intrinsic variability of the carbon fiber diameter and the extremely small amplitude of the capillary forces. The effectiveness of the method was strengthened by fitting the experimental contact angle values by the MKT which permitted to assess the static advancing contact angle as well as the dynamic wetting parameters of the carbon fibers considered in this work.

2 MATERIALS AND METHODS

2.1. Materials

FT300-3000-40A polyacrylonitrile-based carbon fibers manufactured by Toray Carbon Fibers Europe S.A. were used in this study. To obtain clean surfaces, the fibers were washed in ethyl alcohol

and dried at 80ºC for 1h. This gentle cleaning procedure removes dust and grease without altering the sizing that is typically present on commercial carbon fiber. The main properties of the test liquids (n-Hexane: Acros; Deionized water: Millipore Direct Q-3 UV) are listed in Table 1.

Table 1. Liquid/vapor surface tension and density of the probe liquids

Test liquid	¥$_{LV}$ (mN/m)	° (g/cm^3)
n-Hexane	18.4	0.659
Deionized water	72.8	0.98

2.2. Sensitivity of the contact angle measurements.

Advancing and receding contact angles were measured with a high-precision Force Tensiometer – Krüss K100SF (Krüss GmbH, Hamburg, Germany). The instrument was designed to characterize the wettability of single fibers according to the Wilhelmy method [9, 10]. The K100SF tensiometer has a claimed weight resolution of 0.1µg with testing velocities ranging from 0.1mm/min to 500mm/min. During the experiments, a single carbon fiber was attached to the sample holder and set perpendicular to the surface of the test liquid. If standard procedures are followed [11], forces when the fiber is dipped in and then withdrawn from the liquid bath are detected by the microbalance. The fiber is actually not displaced, but the vessel holder moves up (advancing cycle) and down (receding cycle) during the experiments. A sketch of this apparatus is shown in Figure 1.

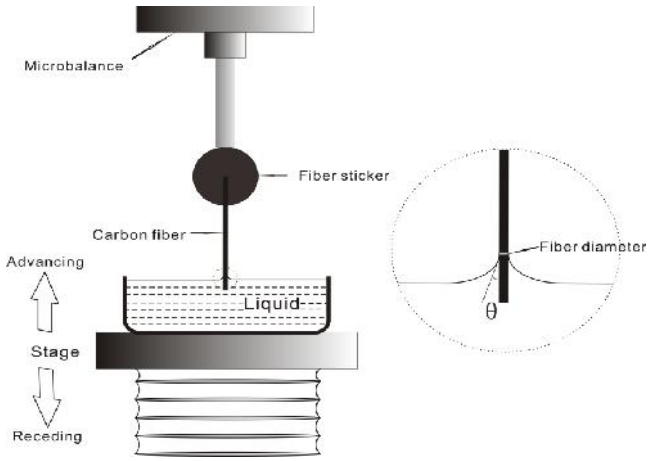

Figure 1.Schematic drawing of the K100 SF tensiometer.

Contact angles at constant advancing and receding velocities can be calculated from: [12]

$$F_{measured} = P¥_{LV}\cos^{-} + mg - F_{buoyancy} \quad (1)$$

where $F_{measured}$ is the force detected by the microbalance, P the perimeter of the fiber, $^{-}$ the dynamic contact angle, m the mass of the fiber, and $F_{buoyancy}$ the buoyancy force. All tests were conducted in monitored and controlled environment (25ºC, 65% relative humidity and soundproof cabinet), so that $¥_{LV}$ is a constant value depending on the test liquid. The calculation of the buoyancy force is based on the density of the test liquid and of the immersed volume of the fiber, $V_{immersed}$.

$$F_{buoyancy} = °gV_{immersed} \quad (2)$$

As low density de-ionized water and hexane were used as test liquids, the buoyancy force is in the order of 10^{-9}mN and can be neglected when compared to the capillary force (the cross section of a single carbon fiber is regarded as circular). The contribution of the weight of the fiber is zeroed at every start of an experiment so that contact angles can simply be calculated by:

$$F_{capillary} = \pi d \gamma_{LV} \cos\theta \quad (3)$$

As γ_{LV} is known in eq 3, θ can be calculated from the capillary force $F_{capillary}$ measured by the tensiometer if the fiber diameter, *d*, is a priori known or measured beforehand. It is common practice to assume that the diameter of regular carbon fibers is about 7µm [13, 14]. Considering such diameter, Figure 2 shows the relation between the capillary force and the calculated contact angle in water (using eq 3).

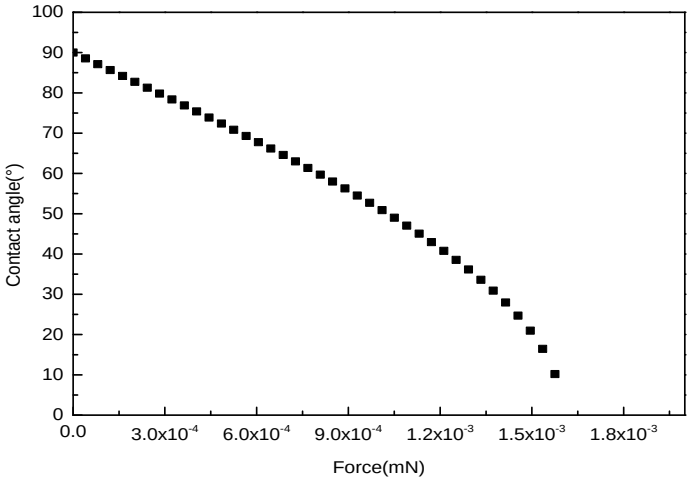

Figure 2.Variation of the contact angle of a single carbon fiber in de-ionized water with a constant diameter of 7µm as a function of the capillary force.

Measuring precise diameters of fibers is also a major prerequisite when calculating contact angles. According to eq 3, when a capillary force is accurately measured by the microbalance, an inaccurate diameter can also lead to erroneous contact angles.

Table 2. Capillary force for carbon fiber/Water system calculated (eq 3) using a reference diameter of 7µm.

Contact angle (º)	80	70	60	40	30	20
Capillary force (mN)	0.00028	0.00055	0.00080	0.00122	0.00139	0.00150

In Figure 3, variations of the contact angle as a function of diameter are compared based on capillary forces given in Table 2. Figure 3 shows that a small variation of the fiber diameter has a significant influence on the contact angle values (for considered angles between 80º and 20º). This trend is amplified when low contact angles are considered (Figure 3b).

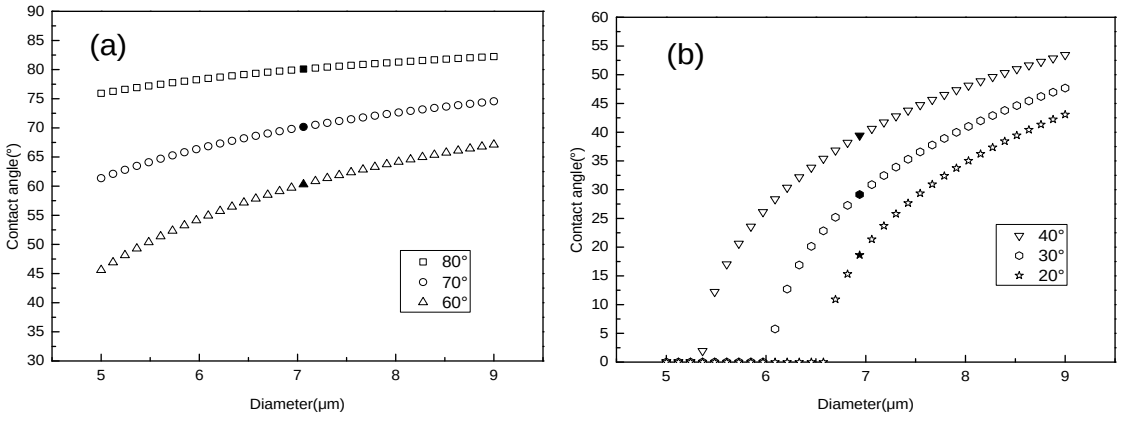

Figure 3. Variation of the contact angle as a function of the diameter of a fiber (keeping the measured force constant): (a) high contact angles and (b) low contact angles.

This simple analysis clearly indicates that a high precision in both the capillary force and the diameter of carbon fibers is required, especially for low contact angles.In this study, a single fiber was tested and a relatively short tested length will help to make sure the single fiber go through the liquid/vapor interface.

2.3. Wetted length measurement.

The K100SF tensiometer was also used to measure the diameter of carbon fibers. The measurements were carried out at room temperature. In this case, n-hexane (99.6%) was the test liquid because it is supposed to perfectly wet the fibers, i.e. θ =0º, leading to a simplified version of the Wilhelmy equation:

$$F_{capillary} = \text{®} d\text{¥}_{LV} \tag{4}$$

The standard procedure to obtain the wetted length or equivalently the fiber diameter is the extrapolation of the immersion force to an immersion depth of 0mm; in this way the buoyancy force can be ignored. Then the first force detected by the tensiometer can be used to calculate the diameter of a single carbon fiber according eq 4. Normally the dynamic tensiometer has a certain detection sensitivity, so that data recording only starts upon contact with the liquid. It was however noted, that with the very small force levels encountered when testing single carbon fibers, various artefacts occurred, causing non-linear and non-steady behavior of the capillary force. Therefore, in this study, the detection sensitivity of the force was set to its minimum value, i.e. 0.1μg, to record forces even before the fiber end is in contact with the liquid surface. Figure 4 shows a typical wetted length measurement curve obtained with n-hexane. The first part (from 0 to 1.7mm) represents the measurement before touching the fluid and highlights a drift in the force. The force level, before touching the fluid, will hereafter be called the “pre-force”. The second part of the curve is related to the capillary process. In standard test protocols, only the second part is normally used to calculate the wetted length. During immersion, the measured force should normally go down due to the buoyancy effect, but it is apparent from Figure 4 that this is not the case here. Therefore, we measured the capillary force in this case from the upward jump in the force at the moment of contact.

The measuring velocity was set to 1mm/min and the maximum rise distance of the stage was 5mm. Then 20 other fibers were selected randomly and measured twice respectively to calculate the average diameter for further comparison with results from SEM.

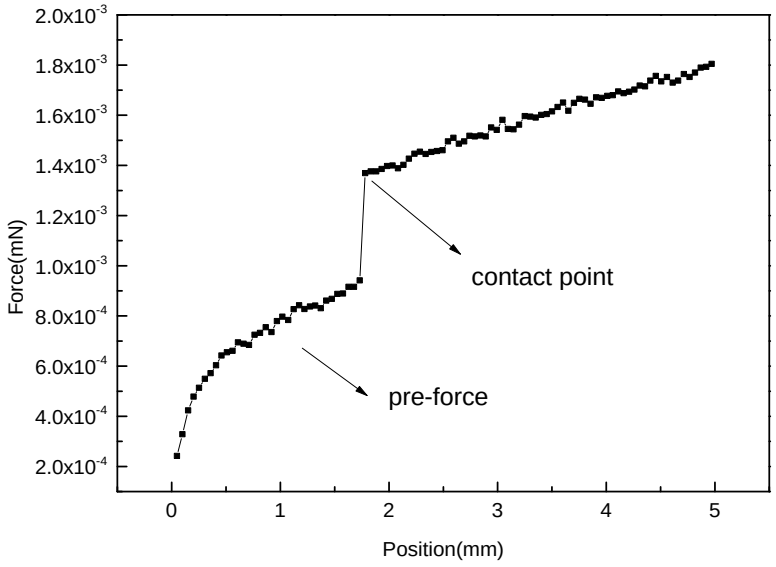

Figure 4.Typical wetted length measurement curve in n-hexane.

2.4. Contact angle measurements.

Once accurate and reliable fiber diameters were obtained and the existence of a drift in the force measured by the tensiometer was analysed, contact angle measurements with deionized water (18.2 $\Omega \cdot$cm resistivity) were implemented. Again, the detection sensitivity was set to its minimum value to trigger the tensiometer before the fiber was in contact with the water/air interface. Every fiber was dipped in and withdrawn from the liquid vessel repeatedly for 3 times at a constant velocity to measure respectively a series of dynamic advancing and receding contact angles. The experiments were conducted at 12 velocities ranging from 0.5mm/min to 500mm/min. 10 fibers with known perimeters were tested per velocity for a total of 120 measurements. The rising distance of the stage was set to 5mm for velocities ranging from 0.5mm/min to 50mm/min and to 20mm for velocities ranging from 100mm/min to 500mm/min to obtain sufficient data.

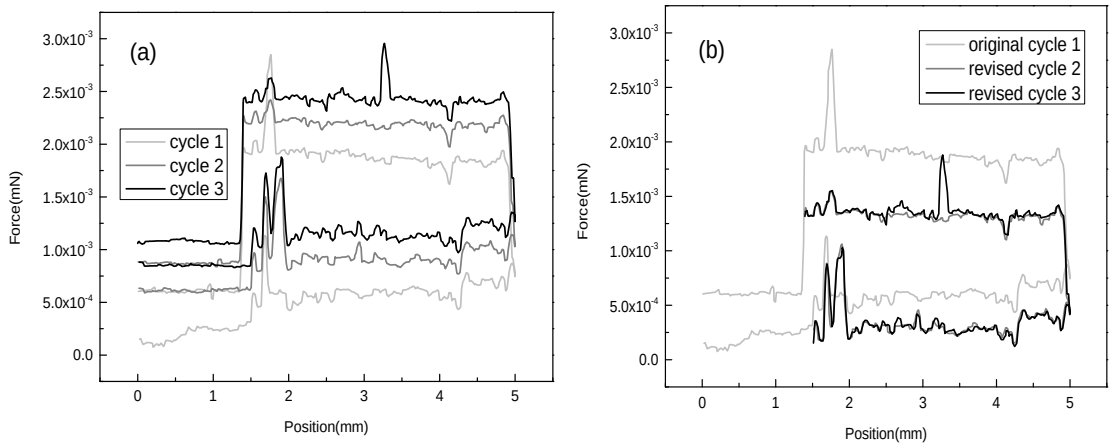

Figure 5. Typical force measurement curves in water: (a) original curves; (b) revised curves.

A typical dynamic contact angle measurement at a speed of 10mm/min is shown in Figure 5a. At the beginning of the first cycle, the force curve initially shows the same kind of upward trend already observed with hexane. After elevating the stage for about 1.5mm, the fiber contacts the water/air interface. The detected force jumps to a higher steady value from which a dynamic advancing contact angle can be measured until a displacement distance of 5mm. The reverse process then takes place (the vessel holder goes down) and a steady receding force can be measured. A stable force is also detected when the fiber moves out of the water. This force, which is higher than the pre-force, is hereafter named "post-force". The initial force of the next cycle (i.e. the pre-force of the 2nd cycle) appears to have exactly the same value as the post-force of the first cycle, as shown in Figure 5a.

The pre- and post-force values were large enough compared to the real capillary forces that they can significantly impact the contact angle values. Therefore, also here a correction was made to the force measured by the tensiometer. For the first cycle, the pre-force goes up for the whole advancing contact angle test process whether the fiber contacts the liquid or not. Due to this, the actual capillary force cannot be evaluated. For the second and third cycle, the amplitude of the pre-force was stable and then subtracted from the force during immersion, see Figure 5b. This way reliable steady advancing contact angles were obtained for carbon fiber in water.

2.5. Scanning electron microscopy (SEM).

After the contact angle measurements, every tested fiber was observed in a FEI XL30 FEG scanning electron microscope to double check the values of the diameters obtained with the K100SF tensiometer. The fibers were dried to remove the water on the surface and then attached by double-sided adhesive tape on the SEM stage. The immersed sections were imaged at a magnification of 5000x under a voltage of 12kV. Three pictures were taken over the length of the immersed sections of the carbon fibers and diameters were measured at 3 different locations for each picture.

2.6. Molecular-kinetic theory (MKT).

To model the contact line motion during wetting, the MKT [6,15] considers a dissipation process occurring close to the contact line where liquid atoms jump on the solid surface from one adsorption site to another. This dissipation is caused by the wetting driving force, i.e. the out-of-balance Young's force $¥_{LV}\left(\cos^{-0}-\cos^{-}\right)$ where $^{-0}$ is the static contact angle [16]. In its general form, the MKT predicts the following relationship between the static and dynamic wetting properties:

$$V = 2©^{0}a \sinh\left[\frac{¥_{LV}a^{2}}{2k_{B}T}\left(\cos^{-0}-\cos^{-}\right)\right] \tag{5}$$

where λ is the atomistic jump length, $©^{0}$ is the atomistic jump frequency, V is the contact line velocity, k_B is the Boltzmann's constant, and T is the temperature (K).

The purpose is here to check if the experimental dynamic wetting data can be modelled by such standard approach [17]. If successful, this fitting procedure would support the experimental methodology and give access to $^{-0}$ [5]. However, it will neither validate the measurements nor the theory as λ and $©^{0}$ are molecular parameters which cannot be measured experimentally. Typical values of around one nanometer for λ and one megahertz for $©^{0}$ are however expected.

3 RESULTS AND DISCUSSION

3.1 Wetted length measurements.

The wetted diameters of 20 carbon fibers obtained from both the tensiometer and SEM are shown in Figure 6. There is a good agreement between the average results obtained from the SEM method (6.83 ± 0.44 μm) and the tensiometer method (7.13 ± 0.44 μm). However, most results of the image analysis are lower than those obtained with the tensiometer. A possible explanation for this variation is that the roughness of the fiber leads to slightly higher perimeters detected by the tensiometer but not reflected by the projected diameters obtained in the SEM. In addition, for the implemented tensiometer method, we only can get local perimeters or diameters. Hence, we selected the diameters obtained from the image analysis technique to calculate the contact angles with water.

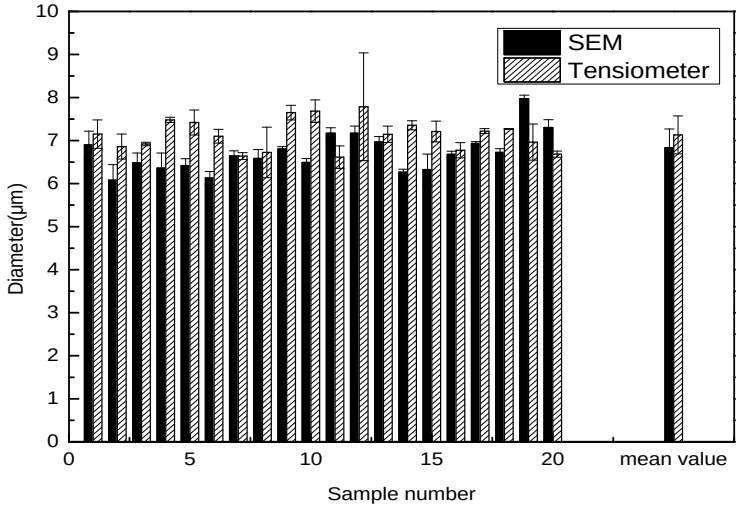

Figure 6.Comparison of carbon fiber diameters obtained from the tensiometer and by SEM.

3.2 Contact angle measurements.

To have a better overview of the wettability of a single fiber, the distribution of contact angles of every tested fiber is then calculated taking into consideration the measurement of the precise wetted perimeter and corrections to the capillary forces obtained from the tensiometer. Dynamic advancing contact angles show finite values, the receding ones have basically values fluctuating between 20º and 0º regardless of the contact line velocity. Figure 7 shows the typical advancing contact angle distributions at the lowest and highest velocities (0.5mm/min and 500mm/min), which were fitted by a Gaussian distribution (eq 6) with the values of the fitted parameters given in Table 3.

$$y = y_0 + Ae^{-\frac{(x-x_c)^2}{2\mu^2}} \tag{6}$$

where x is the advancing contact angle (º), y is the count, y_0 is the offset, x_c is the central position of the peak (º), ω is the width of the distribution, and A is the amplitude of the distribution.

It can be seen that the width of the curves becomes narrower with increasing contact line velocities. This implicates that the distribution of dynamic contact angles is more concentrated at high velocity. An explanation for higher spread at lower velocity is that typically lower contact angles are presented at lower velocities (see e.g. the MKT analysis), which are more easily to be influenced by slight variations of the measured forces or/and wetted length (see section 2.2). Also, all the contact values follow Gaussian distributions which indicate the correctness of the measurements.

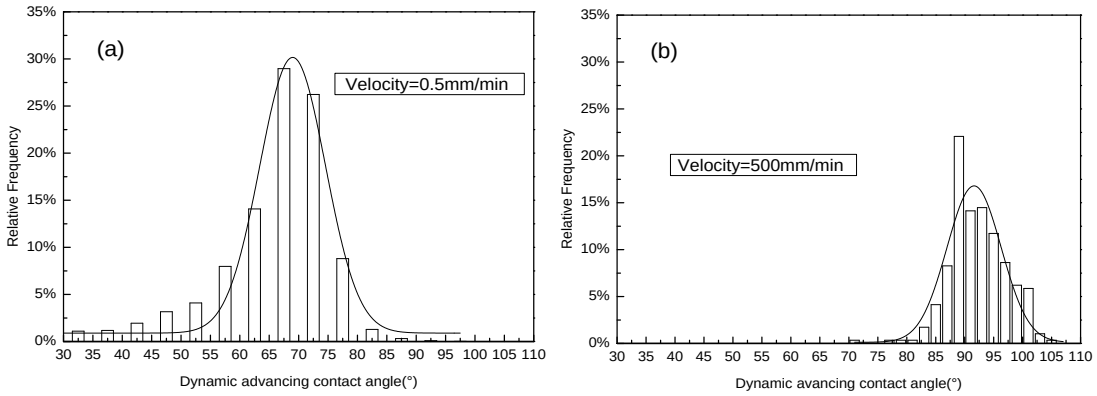

Figure 7.Typical dynamic advancing contact angle distributions: (a) at 0.5mm/min; (b) at 500mm/min.

Table 3. Parameters of distribution fitting for dynamic advancing contact angles.

Velocity(mm/min)	0.5	1	2	5	10	20	50	100	200	300	400	500
Data points	4740	10038	6804	6768	4381	1890	1114	1065	569	473	348	291
x_c(º)	69.0	68.5	71.4	70.7	71.2	73.9	81.2	85.6	88.9	90.4	90.8	91.6
ω	5.6	5.9	4.1	7.3	8.5	7.4	2.6	2.8	3.2	3.5	3.6	4.7
Adj. R-Square*	0.97	0.96	0.97	0.92	0.80	0.71	0.95	0.93	0.98	0.95	0.96	0.85

*Adjusted coefficient of determination which indicates how well data fit a statistical model

After averaging the tested values for each velocity, the dynamic advancing contact angles as a function of the contact line velocity are shown in Figure 8. The contact angles vary from 65.7±10.0º to 92.0±4.8º in water with increasing wetting velocity.

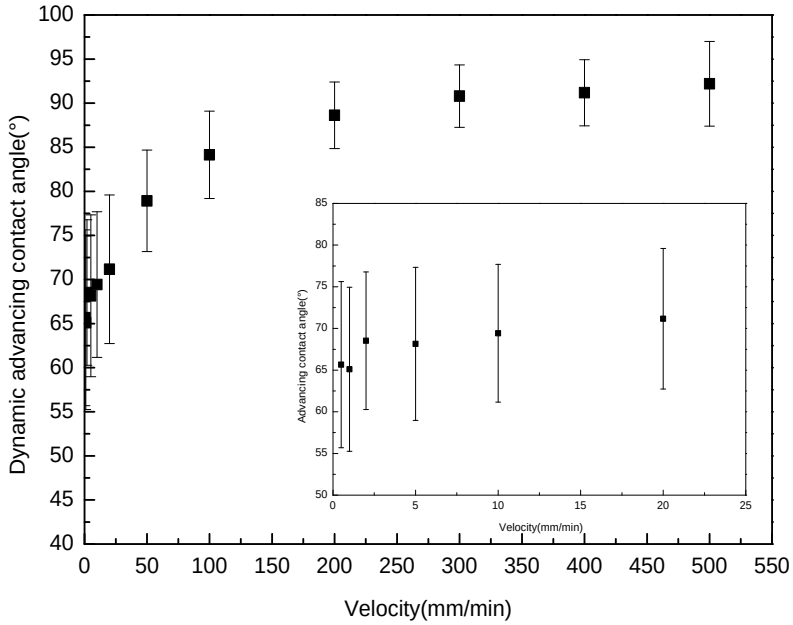

Figure 8.Dynamic advancing contact angle at various measurement velocities. The inset zooms in on the low velocities.

3.3 Dynamic contact angle modelling.

The modelling of the contact angle dynamics was carried out with the G-Dyna software [18] so that the quality of the fit and the distributions of the free parameters, i.e. $©^{0}$, ^{a} and $^{-0}$, can be obtained and their consistency evaluated [2]. Figure 9a shows that the experimental data can be modelled by the MKT quite well. The distributions for ^{a} and $^{-0}$ are narrow whereas the $©^{0}$ values shows a wider distribution (see Figure 9). However, the calculation of a simple average and its associated standard deviation remains meaningful and is presented in Table 4. The model indicates that the dynamic contact angles measured at low velocities, from 0.5mm/min to 20mm/min, are not dissimilar to the static value. It means that dynamic contact angles measured within this range of velocity can be used to calculate the surface energy components of the carbon fibers investigated in this research.

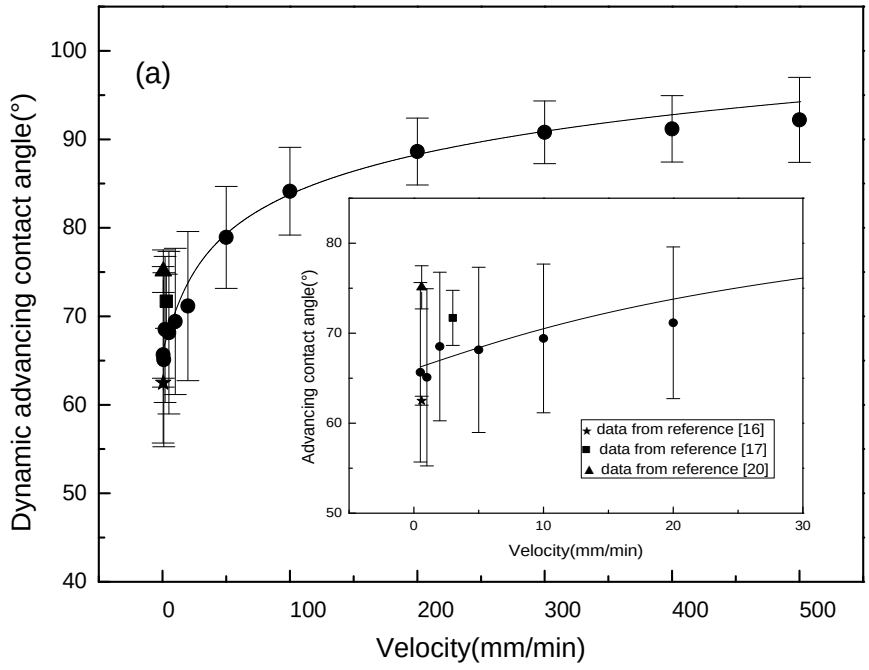

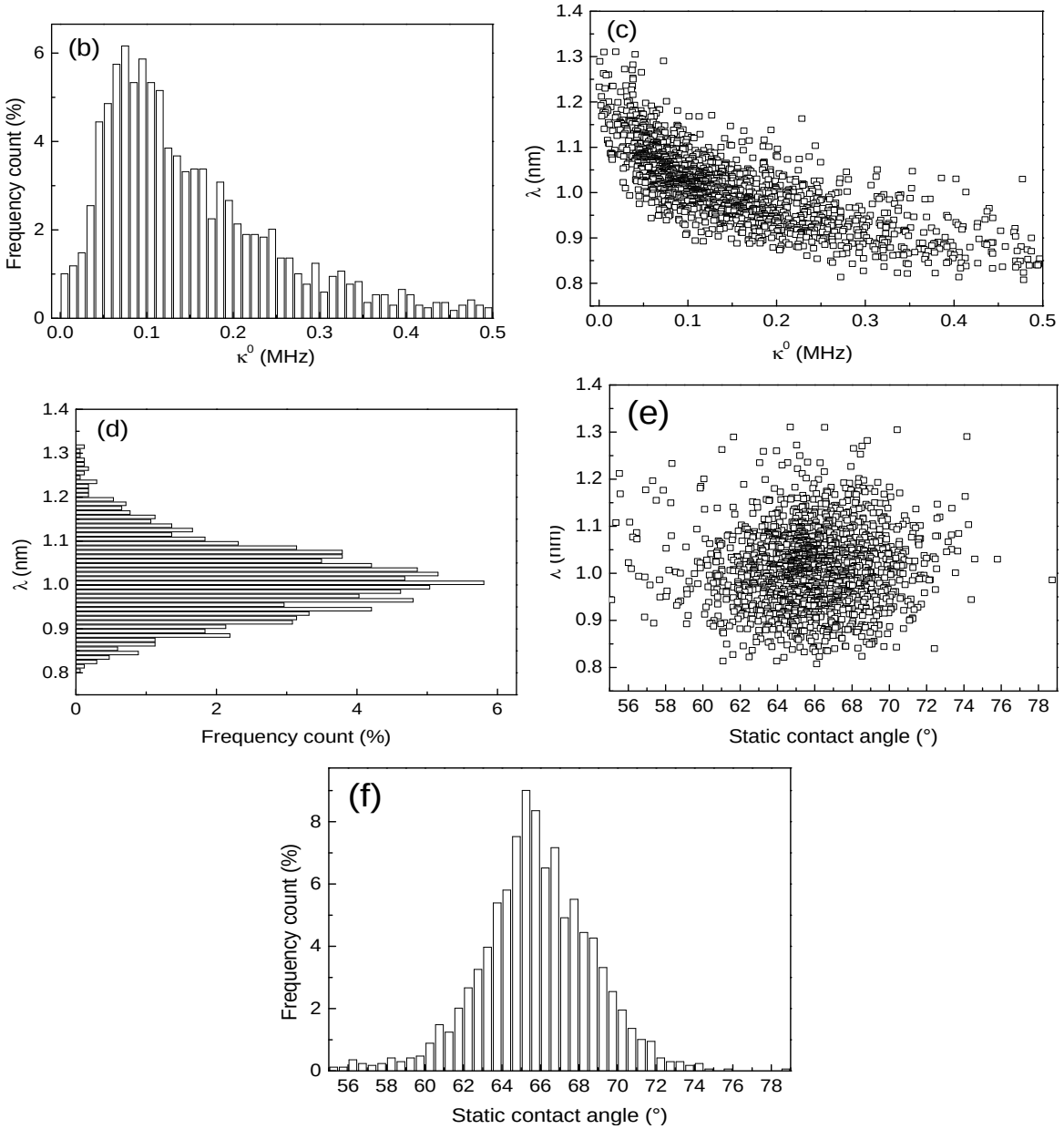

Figure 9. Dynamic advancing contact angle versus contact line velocity fitted by the MKT. (a): Dynamic advancing contact angle versus contact line velocity. Symbols: Experimental data points (this study and other references). Full line: MKT fit. (b): distribution of $©^{0}$. (c): correlation between ^{a} and $©^{0}$. (d): distribution of ^{a}. (e): correlation between ^{a} and $^{-0}$. (f): distribution of $^{-0}$.

Table 4. Average MKT parameters.

Liquid	$©^{0}$	^{a}	$^{-0}$
Water	0.15±0.1MHz	1.0±0.08nm	65.8±2.9º

The MKT fitting is not only a way to model the wetting phenomena but also to show the reliability and accuracy of the presented approach. The MKT provides a good fit to the experimental data, confirming the expected wetting behavior of water on single carbon fiber. The necessary corrections that had to be made to obtain this result, demonstrate that determining wetted length and detected force needs more care when measuring on such fine fibers.

4 CONCLUSION

A new method was developed to measure the dynamic contact angles of a single carbon fiber at low and high velocities (0.5mm/min-500mm/min), taking into consideration both the intrinsic

variability of the carbon fiber diameter and the extremely small amplitude of the capillary forces. SEM analysis confirmed the accuracy of the wetted length measurement by the modified tensiometer method. The amended capillary force ensures the correct measurement of the calculated contact angles. MKT modelling has been used to closely fit the experimental data, demonstrating the effectiveness of the new method and also providing the value of the static contact angle for FT300-3000-40A carbon fiber in de-ionized water (65.8±2.9º). Contact angle values measured at different velocities suggest that dynamic contact angles measured below 20mm/min can be used to calculate the surface energy components of the carbon fibers investigated in this research. In summary, dynamic contact angle tests in water were conducted in a more reliable and accurate way than in previous studies and this will enable better understanding of the wetting behavior of carbon fibers and improve the prospect of employing tensiometry for very fine fibers .

ACKNOWLEDGEMENTS

This work was supported by the Interuniversity Attraction Poles Programme (IAP 7/38 MicroMAST) initiated by the Belgian Science Policy Office and Si Qiu was also supported by the China Scholarship Council scholarships during his stay in KU Leuven.

REFERENCES

[1] Yuan, Y.; Lee, T. R. Contact angle and wetting properties. In Surface science techniques; Springer, 2013, pp 3-34.

[2] Fuentes, C.; Tran, L. Q. N.; Dupont-Gillain, C.; Vanderlinden, W.; De Feyter, S.; Van Vuure, A.; Verpoest, I. Wetting behaviour and surface properties of technical bamboo fibres. Colloids and Surfaces A: Physicochemical and Engineering Aspects 2011, 380 (1), 89-99.

[3] Owen, D.; Wendt, R. Estimation of the surface free energy of polymer. J Appl Polym Sci 1969, 13, 1741-1747.

[4] Van Oss, C. J.; Chaudhury, M. K.; Good, R. J. Interfacial Lifshitz-van der Waals and polar interactions in macroscopic systems. Chemical Reviews 1988, 88 (6), 927-941.

[5] Seveno, D.; Vaillant, A.; Rioboo, R.; Adao, H.; Conti, J.; De Coninck, J. Dynamics of wetting revisited. Langmuir 2009, 25 (22), 13034-13044.

[6] Blake, T.; Haynes, J. Kinetics of liquidliquid displacement. J. Colloid Interface Sci. 1969, 30 (3), 421-423.

[7] Golestanian, H.; El‐Gizawy, A. S. Physical and numerical modeling of mold filling in resin transfer molding. Polym Composite 1998, 19 (4), 395-407.

[8] Park, S.-J. Carbon fibers; Springer2015.

[9] Tran, L. Q. N.; Fuentes, C.; Dupont-Gillain, C.; Van Vuure, A.; Verpoest, I. Wetting analysis and surface characterisation of coir fibres used as reinforcement for composites. Colloids and Surfaces A: Physicochemical and Engineering Aspects 2011, 377 (1), 251-260.

[10] Rhee, K. Y.; Park, S. J.; Hui, D.; Qiu, Y. Effect of oxygen plasma-treated carbon fibers on the tribological behavior of oil-absorbed carbon/epoxy woven composites. Composites Part B: Engineering 2012, 43 (5), 2395-2399.

[11] FK, K., TW Wettability of carbon fibers using single-fiber contact angle measurement-a feasibility study KRÜSS GmbH: Germany2013, pp 1-3.

[12] Yuan, Y.; Lee, T. R. Contact angle and wetting properties. In Surface science techniques; Springer, 2013, pp 3-34.

[13] Xie, J.; Xin, D.; Cao, H.; Wang, C.; Zhao, Y.; Yao, L.; Ji, F.; Qiu, Y. Improving carbon fiber adhesion to polyimide with atmospheric pressure plasma treatment. Surface and Coatings Technology 2011, 206 (2), 191-201.

[14] Li, M.; Gu, Y.; Liu, Y.; Li, Y.; Zhang, Z. Interfacial improvement of carbon fiber/epoxy composites using a simple process for depositing commercially functionalized carbon nanotubes on the fibers. Carbon 2013, 52, 109-121.

[15] Blake, T.; De Coninck, J. The influence of solid–liquid interactions on dynamic wetting. Adv. Colloid Interface Sci. 2002, 96 (1), 21-36.

[16] De Gennes, P.-G. Wetting: statics and dynamics. Reviews of modern physics 1985, 57 (3), 827.

[17] Kim, J.-K.; Mai, Y.-W. Engineered interfaces in fiber reinforced composites; Elsevier1998.

[18] Duvivier, D.; Seveno, D.; Rioboo, R.; Blake, T.; De Coninck, J. Experimental evidence of the role of viscosity in the molecular kinetic theory of dynamic wetting. Langmuir 2011, 27 (21), 13015-13021.